Bulletin of Volcanology (2023) 85:52
https://doi.org/10.1007/s00445-023-01667-8

RESEARCH ARTICLE

U–Pb zircon age and chronology of the Torfufell central volcano: implications for timing of rift relocation in North Iceland

Sigurveig Árnadóttir[1,2] · Thor Thordarson[2] · Árni Hjartarson[3] · Bjarni Gautason[4]

Received: 19 May 2023 / Accepted: 15 August 2023 / Published online: 5 September 2023

Abstract

The Late-Miocene Torfufell central volcano (ToCV), situated between the now extinct Snæfellsnes-Húnaflói rift zone and the presently active rift in North Iceland, provides an excellent opportunity to recreate the construction history of a volcanic edifice. We present new U–Pb zircon ages from six silicic units of the ToCV. The results range from 7.15 ± 0.12 to 6.76 ± 0.02 Ma, taken here to represent a ~ 400 kyr time-span for silicic activity at the volcano. Before that, the central volcano had produced basaltic lavas for 600–800 kyr, implying that it was active for ~ 1–1.2 Myr. A stratigraphically documented ~ 1 Myr hiatus above the volcano is contemporaneous with, but shorter than, a major unconformity in the Flateyjarskagi peninsula, considered to result from a major rift relocation in North Iceland. The new U–Pb ages show that silicic volcanism at the ToCV took place 1–2 Myr earlier than assumed previously and nearly synchronously with the rift relocation. As the age progression of the ToCV and the neighboring 5–6 Ma Tinná central volcano conflicts with the generally established geotectonic framework of central N-Iceland, we propose that these two volcanoes were formed at a leaky transform zone that developed to accommodate the rift relocation, with the ToCV formed at its junction with the embryonic rift zone, thus marking the initiation of the presently active rift in North Iceland. Since then, the two volcanoes have drifted away from the rift system due to plate spreading and migration of the plate boundary relative to the Iceland mantle plume.

Keywords Volcano geology · Geochronology · Iceland · Torfufell · Eyjafjörður · U–Pb zircon age

Introduction

Iceland is situated at the intersection of the Mid-Atlantic Ridge (MAR) and the Iceland mantle plume and is constructed by ridge/plume interaction (e.g., Schilling 1973; Vink 1984). Today, volcanism in Iceland is confined to volcanic zones, each delineated by discrete volcanic systems (e.g., Jakobsson et al. 2008). The volcanic zones are further subdivided into rift-zones, oblique rift-zones (or "leaky" transform zones), propagating rifts and intra-plate belts (e.g., Einarsson 2008). Approximately 30 active volcanic systems are identified within the volcanic zones, and each system features either an elongate fissure swarm, a localized central volcano, or both (e.g., Thordarson and Höskuldsson 2008; Hjartarson and Sæmundsson 2014). The fissure swarms trend subparallel to the respective volcanic zone and typically consist of monogenetic fissures erupting only basaltic magmas, while the central volcanoes are polygenetic (composite) and erupt basaltic to silicic magmas. While a typical lifetime of a volcanic system has been estimated around 0.5–1.5 Myr (Jakobsson et al. 1978; Jakobsson 1979; Sæmundsson 1978; 1979), a lifespan of 2.3–2.4 Myr was evaluated in a recent study for a fossilized volcanic system in East Iceland featuring both a fissure swarm and a central volcano, where the central volcano within the system was active for ~ 1 Myr (Askew et al. 2020). However, central volcanoes in Iceland appear to have potentials for longer lifetimes than that, as longevities of silicic magmatism within individual central volcanoes have been recorded to reach > 1 Myr (Flude et al.

Editorial responsibility: J. Fierstein

✉ Sigurveig Árnadóttir
sigurveig.arnadottir@isor.is

[1] Division of Mapping and Exploration, Iceland GeoSurvey, Akureyri, Iceland

[2] Faculty of Earth Sciences, University of Iceland, Reykjavík, Iceland

[3] Division of Mapping and Exploration, Iceland GeoSurvey, Reykjavík, Iceland

[4] Division of Monitoring and Training, Iceland GeoSurvey, Akureyri, Iceland

2008) and ≥ 1.5 Myr (Banik et al. 2018), with ≥ 2.8 Myr documented as the longest lifespan of silicic activity within an Icelandic central volcano (Carley et al. 2017). Comparably, lifespans of composite volcanoes in other geodynamic settings, such as subduction zones and extensional basins, are commonly estimated around 1–1.3 Myr or less (e.g., Hildreth 2007; Tatsumi et al. 2020; Karaoğlu et al. 2010).

Arrangement of the rift zones in Iceland is explained by the west-northwestward migration of the mid-ocean ridge system in the North Atlantic relative to the Iceland mantle plume, which has induced repeated eastward relocations of the onshore part of MAR-rift segments that are accommodated by transform zones. The present distribution of the rifting segments in Iceland is established by three principal rift zones (Fig. 1a); the ~ N-S trending Northern Volcanic Zone (NVZ) in the north and two subparallel NE-SW trending branches in the south—the Eastern and Western Volcanic Zones (EVZ and WVZ) (e.g., Sæmundsson 1979; Einarsson 2008). These three segments exemplify different stages in the evolution of a rift axis across Iceland, where the southern part of the EVZ is propagating through older crust to the SW, the WVZ is waning and receding, and the NVZ may be referred to as an established (or steady-state) rift as it accommodates the full spreading rate in North Iceland (e.g., Einarsson 2008). The division between the NVZ and the EVZ is nevertheless arbitrary, as these two domains form a single continuous structural identity. Two major transform zones cross Iceland with W-E and WNW-ESE trends: the Tjörnes fracture zone (TFZ) in the north and the South Iceland seismic zone (SISZ) in the south (e.g., Sæmundsson 1979; Jóhannesson 1980). The NVZ is offset towards East from the WVZ along the transverse Mid-Iceland Belt (MIB) which has been described as a "leaky" transform fault (e.g., Óskarsson et al. 1985), i.e., comprising a small component of opening (extension), sufficient to induce local volcanism, although evidence of strike-slip movement in this belt is not apparent (e.g., Hjartardóttir and Einarsson 2021). The extension component has been proposed to be caused by the opposite sense of rotation of crustal blocks to the N and S (Karson 2017). Intra-plate volcanism occurs in the Snæfellsnes and Öræfi Volcanic Belts (SVB and ÖVB), with the former representing renewed volcanism through crust formed in the now extinct Snæfellsnes-Húnaflói rift zone (SHRZ) (Harðarson et al., 1997; Sæmundsson 1979) and the latter considered as an embryonic rift (e.g., Thordarson and Höskuldsson 2002). These intra-plate volcanic zones, along with the propagating part of the EVZ, are typified by alkalic and/or transitional magmatism while the rift zone magmas are tholeiitic (e.g., Jakobsson et al. 2008).

In North Iceland, the last major rift relocation took place when the northern segment of the SHRZ shifted eastward and a new rift axis initiated at the NVZ. The classically quoted timing of the relocation, ~ 6–7 Ma (e.g., Sæmundsson 1979; Jóhannesson 1980), appears to be further supported by new $^{40}Ar/^{39}Ar$ ages from lavas within the Tjörnes sedimentary sequence (Hall et al. 2023). The proposed alignment of the palaeo SHRZ runs along the axis of a syncline (Fig. 1a, b, c), interpreted to be induced by subsidence due to loading of erupted material, causing the volcanic successions to dip towards the then active rift (Sæmundsson 1974; 1979; Jóhannesson 1980; Harðarson et al. 2008). A major discontinuity (unconformity/hiatus) is recorded within the basaltic lava dominated stratigraphical succession along the Flateyjarskagi peninsula, west of the NVZ (Fig. 1b, c). This unconformity is interpreted to have formed because of the rift relocation, where lava flows beneath the hiatus were formed in the SHRZ and lavas above the hiatus were formed in the NVZ (Sæmundsson 1974). Campaigns undertaken to constrain the timing and length of this hiatus indicate that it spans the time from ~ 10 to ~ 6 Ma in the north while the time gap decreases towards the south where it spans the time from ~ 7 to ~ 5 Ma (Jancin et al. 1985; Cotman 1979). These age determinations, along with a number of other datings in central North Iceland (Aronson and Sæmundsson 1975; Sæmundsson et al. 1980; Everts, 1975; Kristjánsson et al. 1992; Fig. 1b, c), were obtained by the K–Ar method which, although certainly useful, has proved to be problematic in Iceland, mostly due to low concentrations of K_2O in Icelandic basalts in combination with problems arising from the mobility of K and resulting sensitivity to the thermal history of the rock. These limitations are largely overcome by the more recent $^{40}Ar/^{39}Ar$ technique (e.g., Lee 2015) which is now considered an optimal method for dating Icelandic rocks (e.g., Sigmarsson et al. 2012). This superseding method has been applied to numerous regional basaltic dykes in central North Iceland, dated in particular to provide spatio-temporal constraints on the ~ 6–7 Ma rift relocation (Garcia et al. 2003). A number of basaltic lavas have also been dated by the $^{40}Ar/^{39}Ar$ method in the central north region, including lavas in Mt. Hólafjall (Supakulopas 2018; Fig. 1b, c; Fig. 2) that provided indications of a major hiatus in the present study area. Age determinations of silicic portions of several of the fossilized and excavated central volcanoes in the central north region of Iceland have furthermore been published, i.e., K–Ar ages from two adjacent volcanoes in the Flateyjarskagi peninsula (Jancin et al. 1985), $^{40}Ar/^{39}Ar$ ages from rhyolite lavas within the Tinná (Hjartarson 2003) and Torfufell (Supakulopas 2018) central volcanoes, and U–Pb zircon ages from intrusive units of the Víðidalur and Laxárdalur central volcanoes (Carley et al. 2020).

The age data mentioned, compiled in Fig. 1b and c, have contributed significantly to the understanding of the volcano-tectonic evolution of central North Iceland, not least by providing constraints on the Flateyjarskagi hiatus and timing of the last major rift relocation in the region. However, a closer look at these ages shows that the distribution

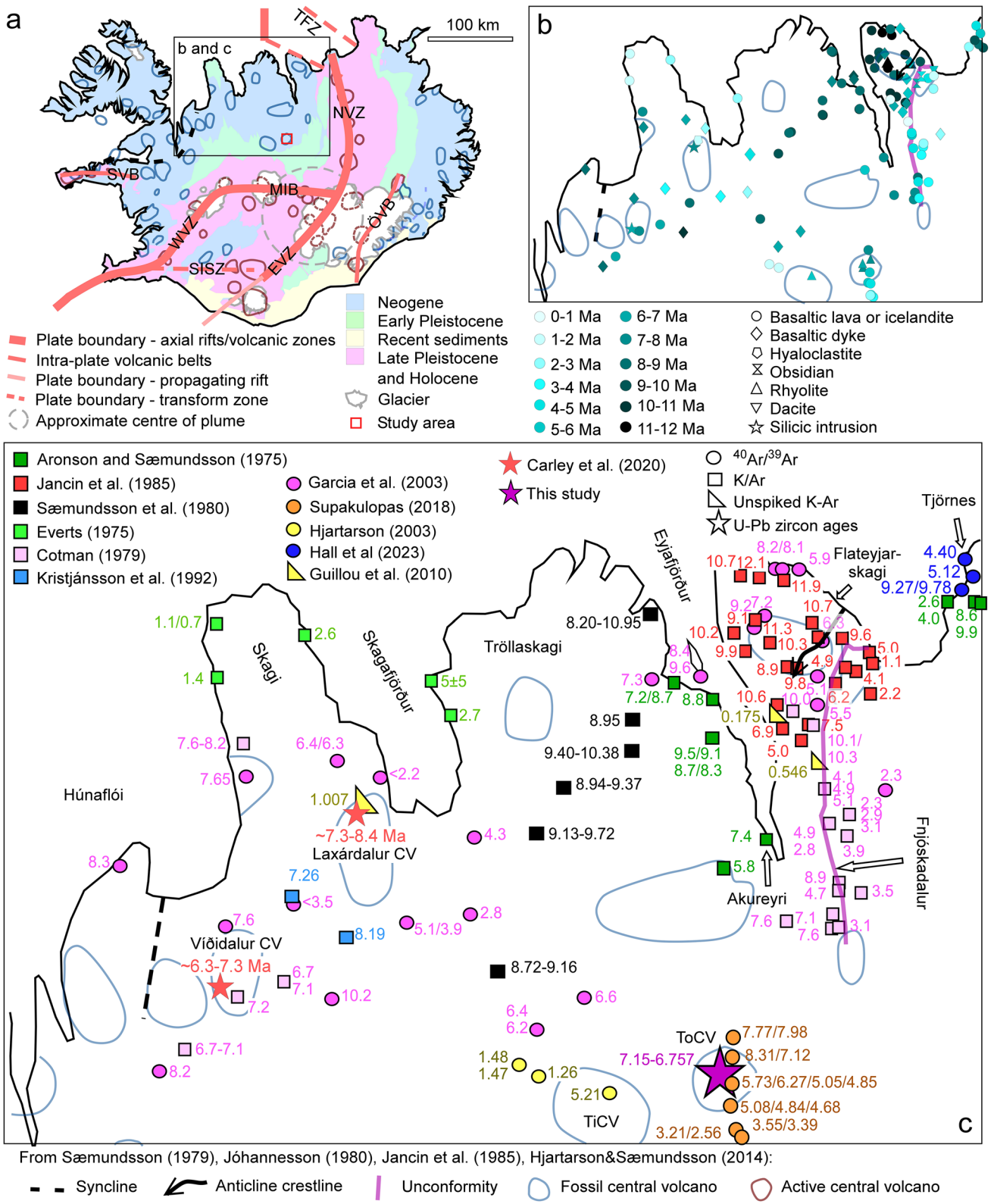

Fig. 1 **a** Generalized geological map of Iceland (modified from Hjartarson & Sæmundsson 2014; Thordarson and Höskuldsson 2008), highlighting active and fossil central volcanoes and active volcanic zones. See text for abbreviations. The approximate center of the Iceland mantle plume, as depicted by Wolfe et al. (1997), is indicated with a gray, dotted circle. **b**, **c** Published radiometric ages from central N-Iceland (compilation aided by Hopper et al. 2014), with features related to the ~ 6–7 Ma rift relocation indicated (i.e., syncline axis, anticline crestline and unconformity); **b** data sorted by age and rock type; **c** data sorted by reference and dating method

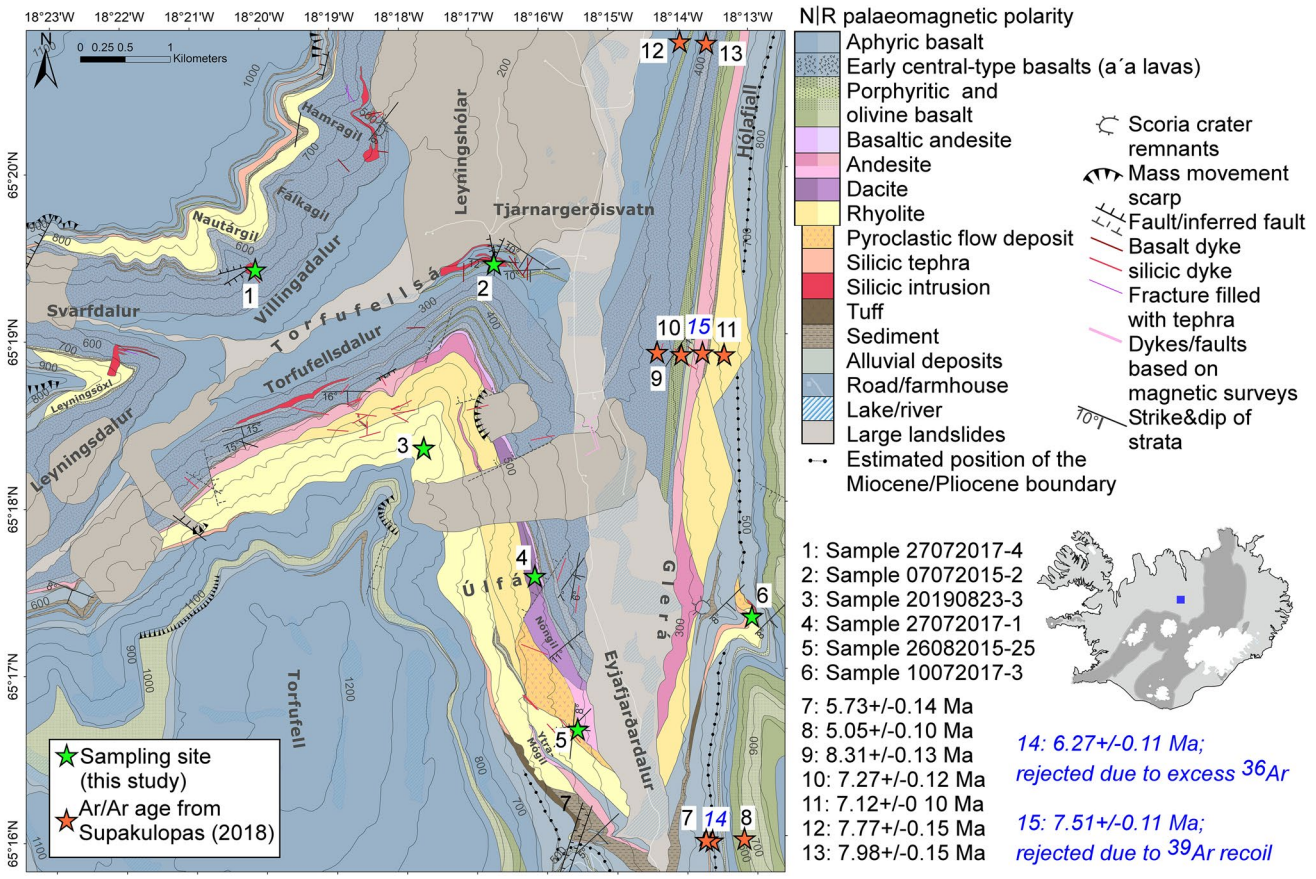

Fig. 2 Sampling sites, shown on a geological map, in comparison with $^{40}Ar/^{39}Ar$ ages in Mt. Hólafjall from Supakulopas (2018). Location of the study area is indicated with a blue box on the small image of Iceland. The geological map is based on original fieldwork, integrated with data from previous authors (stratigraphic and polarity profiles in Mt. Hólafjall from Kristjánsson et al. 2004 and Supakulopas 2018; landslide outlines from Pétursson 1997; dykes/faults based on magnetic surveys from Flóvenz and Tómasson 1992). Basemap: Topography, lakes, rivers, roads and farms sourced from the National Land Survey of Iceland

does not follow a straightforward progression away from the NVZ as assumed for mid-ocean ridge spreading centers. The ages record a general younging to the west, from 12 to 7–7.5 Ma, in the direction away from the Flateyjarskagi unconformity and towards the SHRZ syncline, while lavas above the unconformity are 4–5 Ma. Very young ages are recorded in the Skagafjörður region (Everts 1975; Hjartarson 2003) which have been interpreted as recommenced volcanism, long after extinction of the SHRZ, while lavas of Quaternary age in the Eyjafjörður region have been assumed to be remains of large regional lava flows reaching tens of kilometers out from the NVZ (Guillou et al. 2010). In the Eyjafjörður region (west of the Flateyjarskagi unconformity), a general younging is implied by lava ages from the coastline (i.e., the northernmost Tröllaskagi and Flateyjarskagi peninsulas) and into the land which appears to be non-existent in the western part of the central North region. This younging in the Eyjafjörður region may possibly, at least to some extent, be explained by the general SE dipping of the strata pile (as measured by Jancin et al. 1985) below the Flateyjarskagi unconformity. The apparently non-existent younging from the coastline into the land in the western part of the central North region is unexplained, although it should be noted that in the west, the age data is scarcer than in the east while a large part of the available dates are from dykes instead of lavas. A relatively wide range of ages is recorded in some locations, especially in the Flateyjarskagi peninsula, which may largely be explained by sampling at different stratigraphic levels, while some may possibly be explained by inaccuracy in the K–Ar method.

The primary objective of this study is to address the timing and longevity of silicic ($SiO_2 \geq 65$ wt%) magmatism and volcanism within the Late-Miocene Torfufell central volcano (ToCV), located in the region of the Eyjafjörður fjord, by the Tröllaskagi peninsula's southern end (Figs. 1c and 2), between the presently active NVZ and the northern segment of the palaeo SHRZ. This is a key area in the evolving understanding of rift transfer in North Iceland, allowing us to explore a potential continuation of the Flateyjarskagi unconformity to the south and to examine an inferred

relation of the ToCV with the neighboring Tinná central volcano (TiCV), previously considered to be of similar age and potentially the same volcano (e.g., Hjartarson 2003; 2005). As the ToCV is dissected by rivers and glaciers, it provides an excellent opportunity to recreate the construction history of a volcanic edifice. Contrary to basaltic lavas that may flow tens of kilometers to be observed far away from the eruptive fissure, central volcanoes are localized features, abundantly comprising rocks with restricted spreading such as silicic intrusions and rhyolite lavas of high viscosity and inability to flow long distances, thus providing ages at or very close to the eruptive site. Accordingly, addressing the timing of silicic magmatism of ancient volcanic centers provides geometric relationships that can significantly improve our understanding of the geodynamic evolution of Iceland. Of particular interest are the rhyolites of the Tröllaskagi peninsula which—being situated between the NVZ and the northern segment of the palaeo SHRZ—may hold the key to a more refined comprehension of rift transfer in North Iceland.

This paper details new U–Pb zircon ages from six silicic formations belonging to the ToCV via secondary ion mass spectrometry (SIMS; five formations) and chemical abrasion–isotope dilution thermal ionization mass spectrometry (CA-TIMS; one formation) methods. The SIMS method is a high-spatial resolution in situ technique and was employed in an early stage of the study to obtain, in one batch, a reliable idea about the age of the volcano and its chronological evolution. The CA-TIMS method is a mineral-dissolution technique that results in higher attainable precision than the SIMS method and was employed in a later phase to provide accurate age data for the youngest outcropping rhyolite lava and thereby a more precise conception of the absolute longevity of rhyolite activity at the volcano and, simultaneously, better constraints on the duration of a time gap in the strata pile, indicated by earlier research and supported but abridged by the SIMS age data. The present study was conducted synchronously with field mapping and palaeomagnetic measurements in the study area, with corollary sampling and whole-rock geochemical analyses (detailed separately). In the present paper, we couple the six new U–Pb zircon ages with these observations, as well as with the abovementioned $^{40}Ar/^{39}Ar$ ages from the study area (by Supakulopas 2018), to address the development and life-span of the ToCV and the volcano-tectonic evolution of central North Iceland.

Geological background

The region of the Eyjafjörður fjord is composed of sequences of Neogene flood basalts, commonly interbedded with thin layers of lithified sediments which are typically distinctively red and consisting largely of weathered, wind-blown tephra mixed with ancient soils (Sæmundsson 1979; Sæmundsson et al. 1980; Roaldset 1983). As the originally sub-horizontal lava pile now tilts regionally a few degrees to the south (SW in the northern part, turning to SE in the southern part; Sæmundsson et al. 1980), the oldest lavas occur near the mouth of the fjord while strata from Early Pleistocene are present in the south at the head of the valley Eyjafjarðardalur. Several Miocene central volcanoes have been identified in the region (e.g., Hjartarson and Sæmundsson 2014). Two of these, the Torfufell and Tinná central volcanoes, are ~ 15 km apart and have been proposed to be related and hence of similar age, 5–6 Ma (e.g., Hjartarson 2003; 2005), while Jóhannesson (1991) suggested a higher age for the ToCV than the TiCV, i.e., 6–7 Ma. A stratigraphically constrained ToCV rhyolite yielding $^{40}Ar/^{39}Ar$ age of 7.12 ± 0.10 Ma in Mt. Hólafjall (Supakulopas 2018) indicated an even greater age than both proposals.

The present study area is approximately 40 km south of the largest town in North Iceland, Akureyri (Fig. 1a and Fig. 2). The main features of the bedrock in the area are illustrated in small-scale geological maps of Iceland (e.g., Hjartarson and Sæmundsson 2014), delineating silicic volcanic formations—centered in Mt. Torfufell and enveloped by basaltic lavas—just beneath the boundary between the Miocene and Pliocene periods. Stratigraphic profiling and palaeomagnetic measurements have demonstrated the stratigraphy of Mt. Hólafjall in the eastern part of the area in more detail (Kristjánsson et al. 2004; Supakulopas 2018). Although only partly covering the ToCV, the study by Supakulopas (2018) indicated a ~ 1.5 Ma hiatus between the rhyolite lavas of the ToCV and the overlying basalts.

Field mapping and sample selection

The present study was a part of a field mapping (including stratigraphic and geomagnetic profiling) and geochemical investigation in the area around Mt. Torfufell (detailed separately). The field observations demonstrate that tectonic uplift and glacial erosion has exposed extrusive rocks and shallow intrusions of the ToCV. Outcropping silicic and intermediate extrusive units belonging to the volcano are thickest in the northern part of Mt. Torfufell (Fig. 2), where they form a ~ 400-m-thick succession. The lowermost ~ 30–60 m of this pile are composed of andesite and dacite lavas, which are overlain by thicker rhyolite lavas. Different palaeomagnetic polarities and sediments and individual basaltic to andesitic lavas separating the rhyolite lavas manifest that these are several discrete formations. Below the silicic/intermediate extrusive formations is a 200–300-m-thick stack of basaltic lavas, featuring unusually thin (individual layers typically < 5 m) ā´a lavas. This stack is separated from the silicic/intermediate volcanic

products in several outcrops by a notable tephra-, smectite-, and fossil-bearing sediment horizon. According to our geochemical data, the composition of these unusually thin ā´a lavas is rather evolved and more evolved than underlying plateau basalts (~ 50–52 compared to ~ 48–49 wt% SiO_2; samples 24072017–0 to -3 and 20180903–1 in Table S1 of the Supplementary Material), indicating longer residence time of the magma in the shallow crust. Such unusually thin, phenocryst-free basaltic lava flows have been observed to be abundantly erupted from Icelandic central volcanoes (Sæmundsson 1979) and interpreted to be abnormally thin as they were erupted onto a sloping landscape resulting from the buildup of central volcanism (Walker 1963). Therefore, we have a reason to assume that these thin ā´a lavas below the silicic/intermediate extrusive portion of the ToCV are sourced from the central volcano and erupted during its early phases. Later activity at the central volcano was typified by effusive and explosive rhyolitic eruptions and less frequent and smaller basaltic andesite to dacite events, ceasing with a Plinian eruption. The silicic volcanism was accompanied by silicic intrusions that are exposed at shallow levels (up to ~ 300 m below the base of the silicic/intermediate lavas), with evidence of magma ascending through transgressive sills and erupting through sub-vertical dykes as well as subcylindrical conduits. Basaltic lavas were formed concurrently with the rhyolites and continued to flow alongside the volcanic edifice after the end of silicic activity, eventually burying the highest rhyolitic peaks. A swarm of basaltic dykes is recorded north of the central volcano (north of the map in Fig. 2), but no clear evidence has been observed of whether this dyke swarm belongs to the volcanic system of the ToCV or not. While dykes belonging to this swarm generally trend NNE-SSW, similar to the regional trend of basaltic dykes in the Tröllaskagi peninsula (Sæmundsson et al. 1980), silicic dykes are concentrated in the northern part of Mt. Torfufell, most often striking from ENE-WSW to ESE-WNW. Our strike and dip measurements indicate that the entire strata succession of the study area is dipping gently (from ~ 5 to 11°) towards southeast, while steeper (up to ~ 16°) and more southerly dips (SSE to SSW) are locally indicated in the central zone of the volcanic complex, i.e., in the northern and western slopes of Mt. Torfufell.

Six silicic rock samples from the ToCV were selected, on grounds of the geological mapping and in terms of stratigraphic relations, for U–Pb zircon dating by the SIMS and CA-TIMS methods. Four of the selected samples are from volcanic formations, located at different stratigraphic levels, including samples marking both the base and the top of silicic volcanic products as observed in outcrops. Three of these volcanic formations were formed in effusive eruptions (i.e., lavas) while one is the result of an explosive event (i.e., ignimbrite). The remaining two samples are from intrusive units; one of these is from a sill while the other is from the interiors of a volcanic conduit (plug). Sampling sites are presented in Fig. 2 in comparison with previously published age data from the study area. Descriptions of the six host samples and their stratigraphic levels are presented in Table 1. Our geochemical data, available from 5 of the host samples, indicate that they span a compositional range from ~ 65 to 75% SiO_2. In order to provide background information on the geochemistry of the ToCV, we introduce geochemical analysis results of 27 additional rock samples from the study area (Tables S1 and S2 of the Supplementary Material; detailed separately by Árnadóttir et al., In Prep.). These samples, mostly collected from the central volcano itself while a few are obtained from enveloping lavas, demonstrate that the rhyolites of the ToCV are mildly alkalic, i.e., they have a transitional character towards alkaline rocks, and tend to have high silica contents. The geochemical data show strong similarities with the neighboring TiCV, and a comparison with data from the neovolcanic zones of Iceland indicates that basalt to rhyolite products belonging to these two volcanoes are in general more enriched than typical rift zone magmas (Fig. 3).

Zircons were identified in thin sections of four of the six rock samples; in three samples (07072015–2, 27072017–1, 26082015–25) as inclusions in plagioclase phenocrysts, and in the groundmass of one sample (10072017–3). Nevertheless, it turned out via mineral separation processes that all six host samples featured zircon crystals in different abundances. The highest zircon yield was obtained from samples 10072017–3 and 24072014–4 (~ 120–150 grains per kg rock) while samples 07072015–2, 20190823–3, and 26082015–25 yielded lower abundances (~ 40–70 grains per kg rock). The lowest yield was obtained from the dacite sample, 27072017–1 (~ 16 grains per kg rock). The zircons are commonly ~ 50–200 µm along the c-axis, elongate and prismatic, typically subhedral and less commonly euhedral, and often with pyramidal terminations (see examples in Fig. 4a). Common length-to-width ratios are from 2:1 to 3:1, while some crystals are very long (up to more than 300 µm in length) and thin, with ratios up to 6:1. Cathodoluminescence (CL) images, available from the CA-TIMS dated zircons (20190823–3), do typically not show very distinct brightness variations or strong CL intensities within the crystals as would be expected for well-developed zoning textures indicating distinct growth regions (Fig.S4 of the Supplementary Material). These images do, however, imply zoning in a few crystals and even rounded inherited cores; these crystals were avoided during dating (see examples of dated vs. avoided crystals in Fig. 4a). Only backscattered electron (BSE) images are available from the SIMS dated zircons (Fig.S4 of the Supplementary Material), which are not very helpful for illustrating internal zircon textures. Although test line scans (from energy-dispersive X-ray spectroscopy (EDS) analysis using a scanning electron

Table 1 Descriptions and stratigraphic position of the dated samples

Sample I.D./dating method	Latitude/longitude	Rock type/polarity	Location	Position in the stratigraphy	Sample description
24072017–4/ SIMS	65.321931/ – 18.335686	Intrusion/R	Nautárgil gully in Villingadalur valley	Solidified volcanic plug, exposed ~ 100 m below the base of the silicic portion of the volcano	Light-gray, strongly flow-banded and flaky rhyolite. Aphanitic to glassy groundmass with spherulites and sparse plagioclase phenocrysts
07072015–2/ SIMS	65.324207/ – 18.277519	Intrusion/uncertain	Villingadalsá river gully, southern riverbank	36-m-thick sill, intruded into the basaltic lava pile below the central volcano,. ~ 300 m below the base of the silicic/intermediate horizon within the volcano	Light-gray, very finely grained groundmass featuring high quartz content, plagioclase, Fe-Ti oxides, sparse phenocrysts and small (< 1 mm) vesicles
27072017–1/ SIMS	65.292893/ – 18.268749	Dacite lava/N	Úlfá, east side of Mt. Torfufell	Situated at the base of the silicic/ intermediate horizon of the volcano, resting on top of an evolved basalt lava sequence, representing the early central-volcano basalt succession and overlain by thick rhyolite lavas	Dacitic, flow-banded and flaky lava. Dark-gray aphanitic to glassy groundmass with sparse phenocrysts of plagioclase and clinopyroxene
26082015–25/SIMS	65.277547/ – 18.259066	Ignimbrite/R	Ytra-Mógil, Mt. Torfufell southern part	Among the stratigraphically lowest silicic formations of the volcano; rests on an andesitic flow	Densely welded flow-banded rhyolitic ignimbrite. Aphanitic groundmass tephra with abundant pumice lapilli, lithics, and phenocrysts (mostly plagioclase)
10072017–3/ SIMS	65.288856/ – 18.218619	Rhyolite lava/R	Glerá gully, Mt. Hólafjall southern part	Small patch of rhyolite, assumed to be an edge of a larger lava dome. Formed during later stages of silicic volcanism; overlies some of the basaltic lavas that adjoin older rhyolite domes	Flaky and flow-banded rhyolite lava. Aphanitic to glassy groundmass of quartz, alkaline feldspar, and opaque minerals; altered, often spherulitic. Sparse plagioclase phenocrysts
20190823–3/ CA-TIMS	65.305372/ – 18.294526	Rhyolite lava/R	Mt. Torfufell northern part	The topmost rhyolite lava present in Mt. Torfufell, marking the top of the silicic horizon within the volcano	Flaky rhyolitic lava. Aphanitic, light-gray groundmass

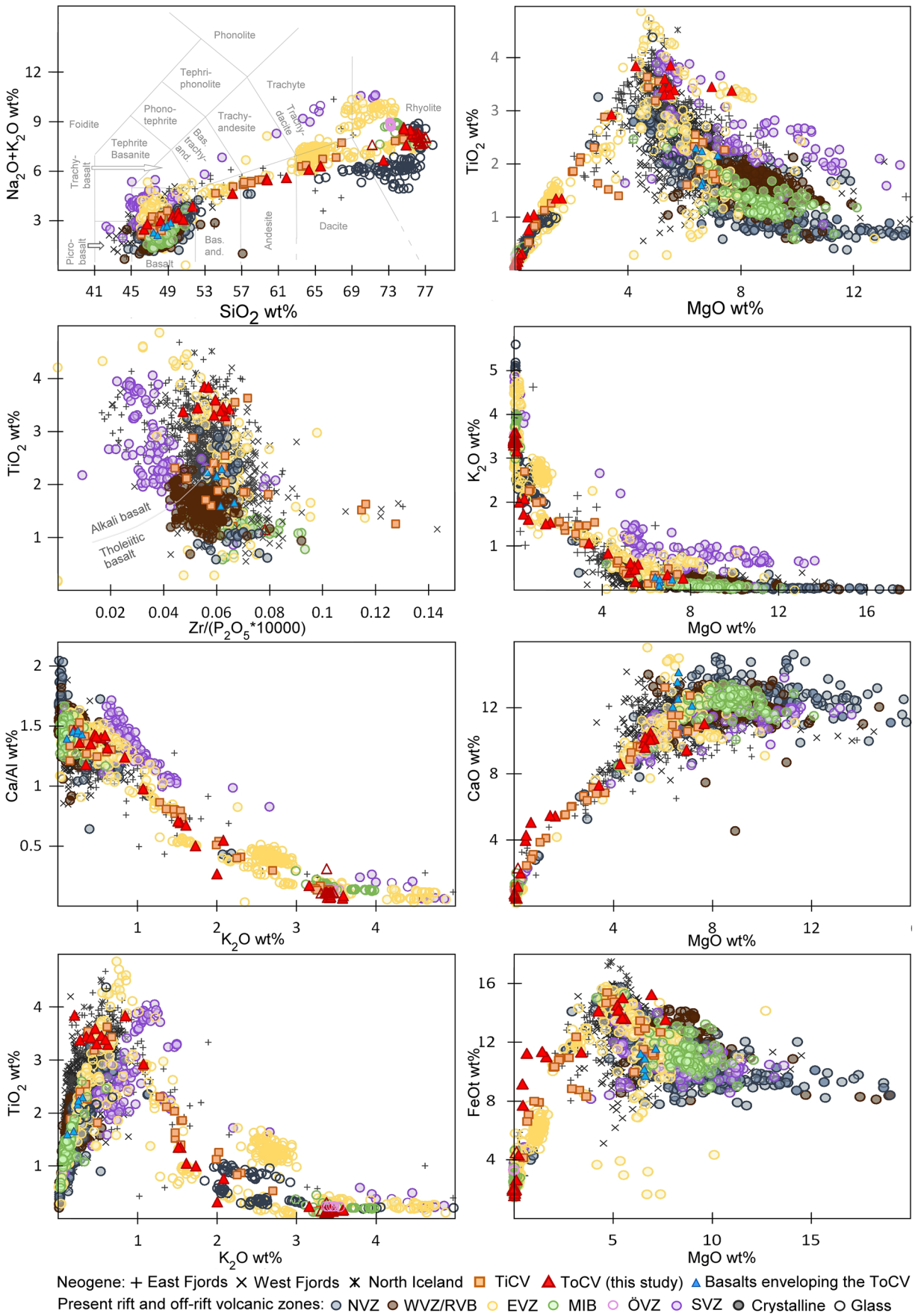
Phonolite
Tephri-phonolite
Trachyte
Phono-tephrite
Trachy-andesite
Rhyolite
Foidite
Tephrite Basanite
Bas. trachy-and.
Trachy-dacite
Trachy-basalt
Andesite
Dacite
Picro-basalt
Bas. and.
Basalt
Na2O+K2O wt%
SiO2 wt%
TiO2 wt%
MgO wt%
Alkali basalt
Tholeiitic basalt
Zr/(P2O5*10000)
K2O wt%
Ca/Al wt%
CaO wt%
FeOt wt%
Neogene: East Fjords West Fjords North Iceland TiCV ToCV (this study) Basalts enveloping the ToCV
Present rift and off-rift volcanic zones: NVZ WVZ/RVB EVZ MIB ÖVZ SVZ Crystalline Glass

◂**Fig. 3** Geochemistry of the ToCV in comparison with samples from the neovolcanic zones in Iceland, the TiCV and the Neogene East and West fjords. The samples dated in this study are signified with bright red diamonds. Comparison data is from Clay et al. (2015), Debaille et al. (2009), Fitton et al. (1997), Flude et al. (2010), Fowler and Zierenberg (2016), Guðmundsdóttir et al. (2011), Gunnarsson et al. (1998), Harðarson (1993), Hardarson and Fitton (1997), Hardarson et al. (1997), Hjartarson (2003), Kuritani et al. (2011), Lacasse et al. (2007), Larsen et al. (1999; 2001; 2002), Maclennan et al. (2001), Martin and Sigmarsson (2007), Mattsson and Óskarsson (2005), McGarvie et al. (1990; 2007), Meara et al. (2020), Nicholson et al. (1991), Óladóttir et al. (2011), Pollock et al. (2014), Selbekk and Trönnes 2007, Sigvaldason (1979), Sinton et al. (2005), Slater (1996), Slater et al. (2001), Viccaro et al. (2015), and Zierenberg et al. (2013). The total alkali-silica diagram (TAS; uppermost left) shows root names from Le Bas et al. (1986). The TiO_2 vs $Zr/(P_2O_5 \times 10{,}000)$ plot shows the discrimination between alkali basalts and tholeiite basalts after Winchester and Floyd (1976)

microscope (SEM)) through cross-sections of several randomly selected zircons indicate that distribution of elements within the crystals is rather homogeneous (see example in Fig. 4b), it cannot be excluded that some of the SIMS dated zircons have inherited domains. In order to reduce the influence of such domains, the zircon cores were avoided as much as possible during dating. Inclusions of other minerals are rather commonly observed in zircons from all samples (see example in Fig. 4b); these were also evaded during dating.

Analytical methods

Secondary ion mass spectrometry

U–Pb dating of zircons from host samples 20172017–1, 26082015–25, 07072015–2, 24072017–4, and 10072017–3 was carried out via in situ measurements using the CAMECA ims 1280 in the NordSIMS facility, Swedish Museum of Natural History, Stockholm. Zircons were separated from these five host samples using standard crushing, sieving, and density and magnetic methods by Geotrack in Australia. The zircon grains were mounted by hand onto a two-sided tape along with reference materials and then epoxy-casted and polished to expose grain interiors. The polished mount was imaged using backscattered electron signals in SEM (Hitachi TM3000 SEM at the University of Iceland) in order to carefully map the sample mount prior to dating, to confirm zircon identities of crystals, and to identify internal structures such as inclusions and cracks that were avoided during the dating. The zircon cores were also avoided during dating in order to exclude potential inheritance as possible.

The analytical and calibration procedures generally followed those described in Whitehouse and Kamber (2005) and Jeon and Whitehouse (2015), with a few differences noted in Supplementary Text S1. In total, 97 U–Pb analyses were carried out on 92 zircon grains from the five samples (all analyzed spots are presented in Fig.S4 of the Supplementary Material) and thereof, 7 analyses were excluded, resulting in a total of 90 analyzed spots. Eleven grains were selected from sample 27072017–1 (12 spots; thereof 2 spots were discordant and excluded (assumed as contamination due to abnormally high age; 529 and > 1200 Ma)); 19 grains from sample 26082015–25 (21 spots; thereof 2 spots were discordant and excluded (assumed as contamination due to abnormally high age; 73 and > 1200 Ma)); 22 grains from 07072015–2 (22 spots; no spot excluded); 21 grains from 24072017–4 (21 spots; no spot excluded); and 19 grains from 10072017–3 (21 spots; thereof 3 spots were excluded due to outstandingly high common Pb).

Chemical abrasion–isotope dilution thermal ionization mass spectrometry

Zircons from host sample 20190823–3 were dated at the Pacific Centre for Isotopic and Geochemical Research (PCIGR) at the University of British Columbia (UBC) by CA-TIMS method. The sample was prepared at the PCIGR, including separation of zircon crystals from the host sample and CL SEM imaging. Zircon crystals were subjected to a pre-treatment combining annealing and a modified version of Mattinson's (2005) chemical abrasion method for removing zircon domains that have lost lead from the interior of grains (see Supplementary Text S1). By this, the CA-TIMS method can isolate and analyze closed-system, high-quality domains within the zircon grains and exclude discordance due to loss of lead. The mineral-dissolution method furthermore samples larger volumes of material than the SIMS method, resulting in higher attainable precision. Prior to the chemical abrasion, 33 zircon grains were selected for in situ determination of trace element concentrations by LA-ICPMS (the LA-ICPMS conditions are given in Supplementary Table S7; the method is described in Supplementary Text S1). Six zircon grains were then selected for CA-TIMS analysis based on the LA-ICPMS results in combination with the prismatic morphology and the absence of inclusions, avoiding those crystals with rounded edges. U–Pb geochronology methods for isotope dilution thermal ionization mass spectrometry follow those previously published by Wall et al. (2018), detailed in Supplementary Text S1. Chemical abrasion in concentrated HF at 190° for 12 h resulted in only minor dissolution of the zircon crystals.

Results

Our U–Pb zircon ages (weighted averages) range from 7.15 ± 0.12 to 6.76 ± 0.02 Ma (error is in 2σ); that is Late Miocene. Weighted mean ages for each sample are

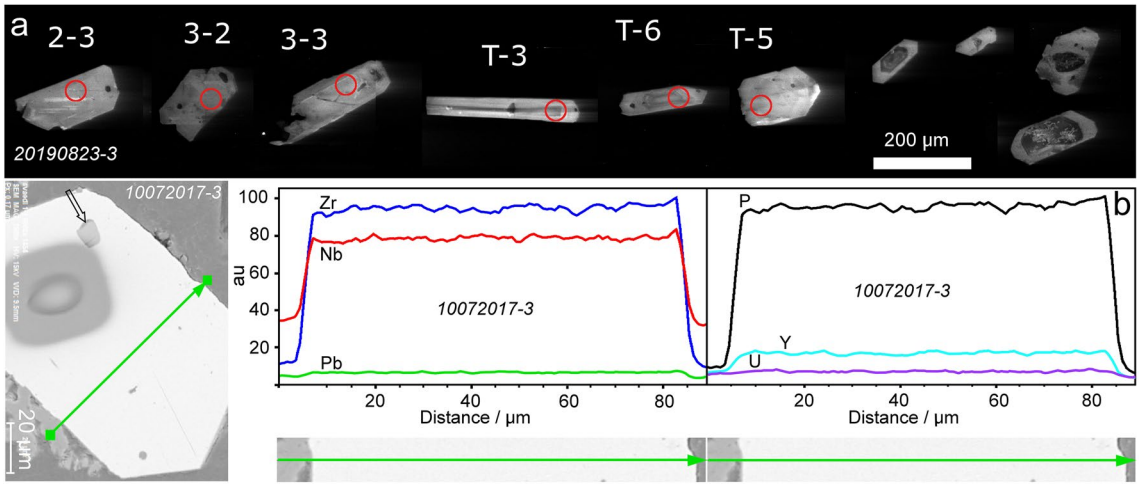

Fig. 4 **a** CL images of zircons from sample 20190823–3. Numbered zircon grains were dated with the CA-TIMS method (with red circles indicating location of laser ablation inductively coupled plasma mass spectrometry (LA-ICPMS) spots) while zircons without numbers (and without red circles) are examples of avoided grains. **b** Example of a random line scan test (from EDS analysis using a SEM) through a cross-section of a zircon dated with the SIMS method (au = arbitrary units). The alignment of the line scan is shown to the left. The large dark area inside the crystal is a spot/crater generated by the defocused beam during SIMS dating. A ~ 10 µm inclusion, observed next to the spot (indicated with an arrow) is rich in Ca and rimmed by Al- and Si-rich material

Table 2 Summary of U–Pb radiometric data. Ages are given as weighted averages. Detailed results are listed in Tables S3 and S4 in the Supplementary Material

Sample ID	Rock type	Weighted average U–Pb age (Ma)/*TuffZirc age (Ma)*	2σ	Method	Number of dated grains/analyzed spots	MSWD
24072017–4	Volcanic plug	7.015	±0.048	SIMS	21/21	1.13
07072015–2	Silicic sill	7.002	±0.064	SIMS	22/22	1.5
27072017–1	Dacite lava	7.03	±0.15	SIMS	9/10	1.8
26082015–25	Ignimbrite	7.15/*7.03*	±0.12/+*0.18–0.07*	SIMS	17/19	4.3
10072017–3	Rhyolite lava	6.85/*6.93*	±0.091/+*0.08–0.1*	SIMS	17/18	5.1
20190823–3	Rhyolite lava	6.757	±0.015	CA-TIMS	6/N.A	0.98

presented in Table 2 and Fig. 5a, while detailed results are listed in Tables S3-S4 and Figures S1-S4 of the Supplementary Material. Results of LA-ICPMS U-(Th-)Pb and trace element analysis of zircons from sample 20190823–3 are given in Tables S5-S6 of the Supplementary Material. Very similar ages were obtained for the two intrusive units, showing an age of 7.00 ± 0.06 Ma for the sill (sample 07072015–2) and 7.02 ± 0.05 Ma for the volcanic plug (sample 24072017–4). Slightly higher ages were obtained for the early silicic extrusive units: 7.03 ± 0.15 Ma for the dacite lava (sample 27072017–1) while the highest obtained U–Pb mean age is the ignimbrite age, 7.15 ± 0.12 Ma (Sample 26082015–25), although located slightly higher in the stratigraphy than the dacite. The ages of the upper rhyolite lavas are 6.85 ± 0.09 Ma for the Glerá lava (sample 10072017–3) and 6.76 ± 0.02 Ma for the uppermost rhyolite in Mt. Torfufell (sample 20190823–3). Very low 2σ and mean square weighted deviation (MSWD) were obtained for the CA-TIMS dated sample compared to the SIMS dated samples. Four SIMS analyses were rejected to get statistically meaningful MSWD (a value under 2) and probability (higher than 0.05 for 95% confidence level), 2 rejections in 07072015–2, 1 in 27072017–1 and 1 in 26082015–25 (blue bars in Fig. 5a and Fig.S2 of the Supplementary Material). However, while MSWD is < 2 for most SIMS samples, high MSWDs (> 4) were obtained for two samples (26082015–25 and 10072017–3). The weighted averages of these two samples also have zero probability, meaning that their data are too scattered to get a statistically grouped age—and the probability density plots for these two samples show more than one peak (while the plots for the other samples show a single peak), indicating that the data from each sample consists of more than one population (Figures S2 and S3 of the Supplementary Material). Since the zircons are young and fairly low in U, it is not reasonable to assign this to Pb loss, as might be the case for older and/or U-rich zircons.

Instead, we rather assume that the dispersion in these two samples is related to recycling/mixing of older zircons into younger melts. To improve the situation, the data from these two samples were processed using the *TuffZirc* algorithm of Isoplot, which is largely insensitive to both Pb loss and inheritance and looks at the data statistically for a coherent group (Ludwig and Mundil 2002; Ludwig 2003). The ages calculated by *TuffZirc* are $7.03+0.18/-0.07$ Ma for sample 26082015–25 (95.1% conf, from a coherent group of 12) and $6.93+0.08/-0.1$ Ma for sample 10072017–3 (93.5% conf, from a coherent group of 11; Fig. 5a and Fig.S3 of the Supplementary Material).

Discussion

The silicic samples selected for this study are from volcanic formations, located at different stratigraphic levels, and intrusive units of the ToCV. By this, we were able to provide geochronological data that can be interpreted to represent the age range of silicic magmatism and volcanism at the volcano. We base the timing of the initiation of the ToCV on Supakulopas's (2018) $^{40}Ar/^{39}Ar$ 7.77 ± 0.15 and 7.98 ± 0.15 Ma ages, obtained from samples collected above and below the stratigraphic level of the base of the pile of thin basaltic ā'a lavas that we assume to define the onset of eruptions at the central volcano (Fig. 5a). However, as these two ages are inconsistent to the stratigraphic order (i.e., the higher age was obtained for the lava that is located higher in the strata pile while the lower lava gave younger age), the estimated timing of the establishment of the edifice base is quite imprecise (therefore given here as ~ 7.8–8.0 Ma). While no age determinations are available for intermediate formations, correlation with Supakulopas (2018) and the geomagnetic time scale provides a rough estimate, indicating that intermediate volcanism began during geomagnetic subchron C3Br.2r (i.e., somewhere on the range from ~ 7.3 to ~ 7.5 Ma; Ogg 2020).

Our oldest weighted average U–Pb age (7.15 ± 0.12 Ma) was obtained for the ignimbrite sample (26082015–25), which appears to be located higher in the strata pile than the younger dacite sample (27072017–1; 7.03 ± 0.15 Ma). As the MSWD for the ignimbrite sample is high (4.3), and as the probability density plot for this sample indicates that the data consists of more than one population (Fig.S3 of the Supplementary Material), it may be speculated that there is an older (~ 7.4 Ma) component in a ~ 7 Ma melt that could explain the higher weighted average U–Pb age, suggesting that the ignimbrite and the dacite were emplaced in close temporal proximity. The $7.03+0.18/-0.07$ Ma age of the ignimbrite, extracted from the most-coherent population by the *TuffZirc* algorithm of Isoplot (Ludwig and Mundil 2002; Ludwig 2003), supports this idea (Fig. 5a and Fig.S3 of the Supplementary Material). The older component in the ignimbrite may e.g., be derived from zircon inclusions in plagioclase phenocrysts, and/or from silicic lithics in the whole-rock sample, which would imply silicic magmatism as early as 7.4 Ma at the ToCV. However, as Supakulopas's (2018) 7.12 ± 0.10 Ma $^{40}Ar/^{39}Ar$ age is from the lowermost rhyolite lava in Mt. Hólafjall, it can be considered to approximately mark the onset of silicic volcanism at the ToCV.

The two youngest weighted average ages, 6.85 ± 0.09 and 6.76 ± 0.02, are from lavas representing late silicic volcanism at the ToCV (samples 10072017–3 and 20190823–3, respectively). The weighted average of sample 10072017–3 has zero probability; MSWD for this sample is high (5.1) and the relative probability plot indicates that the data consists of more than one population (~ 7.0 and ~ 6.8 Ma; Figures S2 and S3 of the Supplementary Material). The most-coherent group of zircon ages, determined using the *TuffZirc* algorithm of Isoplot (Ludwig and Mundil 2002; Ludwig 2003), provided an age of $6.93+0.08/-0.1$ Ma (Fig. 5a and Fig.S3 of the Supplementary Material). While this sample is not confidently assigned to the youngest rhyolite lava at the volcano, sample 20190823–3 is collected at the highest rhyolite peak and has MSWD very close to 1 (0.98), showing decidedly that silicic activity continued at the ToCV until 6.76 ± 0.02 Ma. Field relations indicate that the rhyolite activity was succeeded by regional basaltic volcanism. Supakulopas (2018) provided a 5.73 ± 0.14 Ma age for a basaltic lava onlapping a rhyolite formation in Mt. Hólafjall which, according to his interpretation, was formed during geomagnetic subchron C3Bn (~ 7.21–7.10 Ma), thereby identifying a ~ 1.5 Myr hiatus between these sequences (Fig. 5a). This hiatus is somewhat shortened by at least four lavas that are present between these two units, and due to the palaeo-landscape, the length of the hiatus may vary within the area, probably increasing in length at the highest rhyolite peak. Nevertheless, as we date the youngest rhyolite at 6.76 ± 0.02 Ma, it may be assumed that ~ 1 Myr passed from the extinction of the ToCV until basaltic lavas from nearby fissure swarms began to onlap the volcano.

The available age data indicate that the ToCV was active from ~ 7.8–8.0 to 6.76 ± 0.02 Ma, or for ~ 1–1.2 Myr, and that silicic magmatism and volcanism occurred during the last ~ 0.4 Myr of the volcano's life-span. Consistent with Supakulopas' (2018) conclusions, our age data show that the silicic rocks of the ToCV are 1–2 Myr older than suggested by earlier researchers (e.g., Hjartarson 2003; 2005). The longest hiatus in the research area appears to be between the volcano's uppermost rhyolites and the younger, succeeding basalts. Although relatively shorter than the time gap recorded in the Flateyjarskagi peninsula, it may be speculated if the hiatus observed above the ToCV is potentially an extension of this major unconformity and thereby related to a plate boundary shift. If so, and according to the general

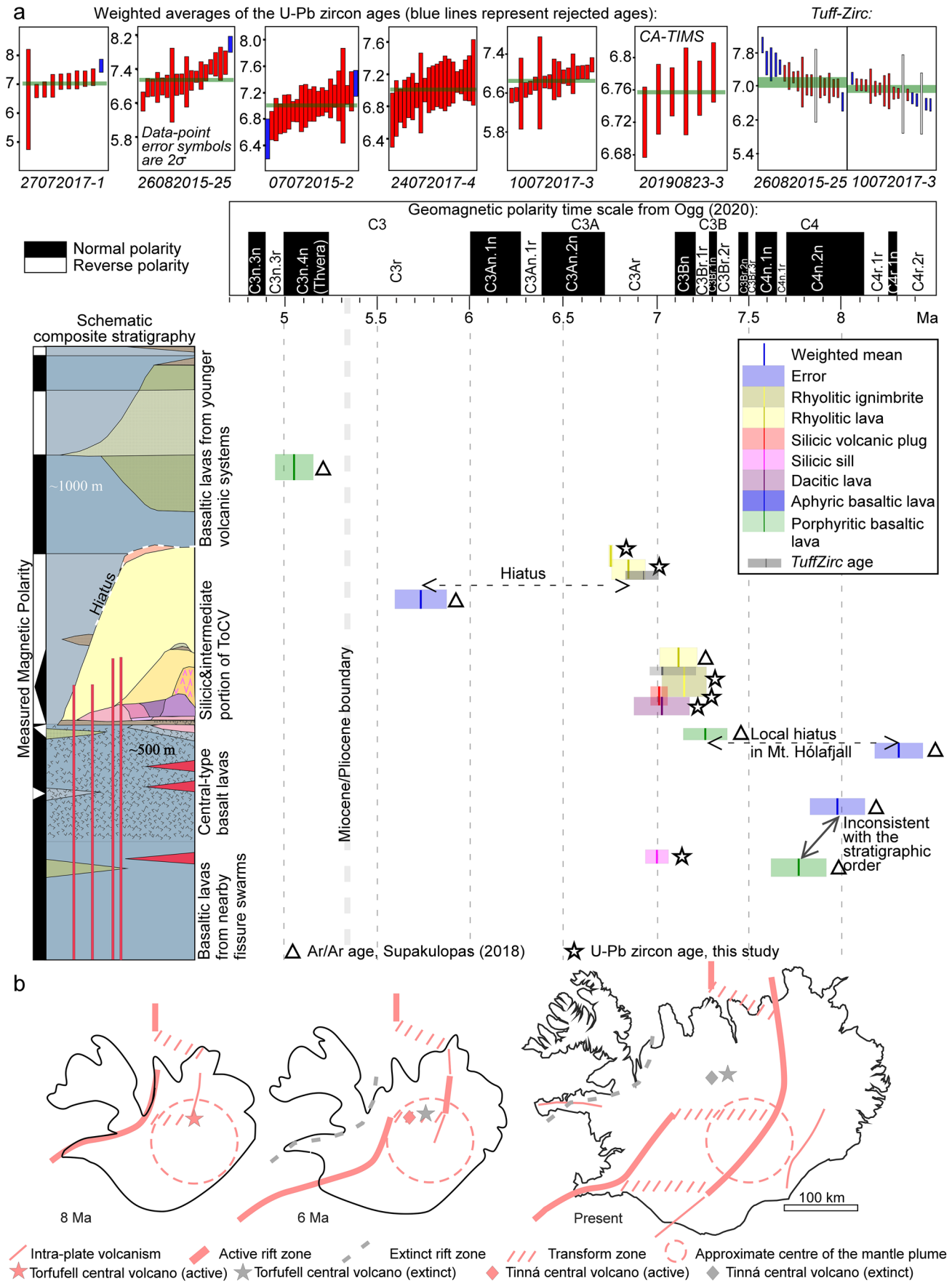
a
Weighted averages of the U-Pb zircon ages (blue lines represent rejected ages):
Tuff-Zirc:
CA-TIMS
Data-point error symbols are 2σ
27072017-1
26082015-25
07072015-2
24072017-4
10072017-3
20190823-3
26082015-25 10072017-3
Geomagnetic polarity time scale from Ogg (2020):
Normal polarity
Reverse polarity
C3
C3A
C3B
C4
C3n.3n
C3n.3r
C3n.4n (Thvera)
C3r
C3An.1n
C3An.1r
C3An.2n
C3Ar
C3Bn
C3Br.1r
C3Br.2r
C4n.1n
C4n.2n
C4r.1r
C4r.2r
Ma
Schematic composite stratigraphy
~1000 m
~500 m
Hiatus
Measured Magnetic Polarity
Basaltic lavas from younger volcanic systems
Silicic&intermediate portion of ToCV
Central-type basalt lavas
Basaltic lavas from nearby fissure swarms
Miocene/Pliocene boundary
Weighted mean
Error
Rhyolitic ignimbrite
Rhyolitic lava
Silicic volcanic plug
Silicic sill
Dacitic lava
Aphyric basaltic lava
Porphyritic basaltic lava
TuffZirc age
Hiatus
Local hiatus in Mt. Hólafjall
Inconsistent with the stratigraphic order
Ar/Ar age, Supakulopas (2018)
U-Pb zircon age, this study
b
8 Ma
6 Ma
Present
100 km
Intra-plate volcanism
Active rift zone
Extinct rift zone
Transform zone
Approximate centre of the mantle plume
Torfufell central volcano (active)
Torfufell central volcano (extinct)
Tinná central volcano (active)
Tinná central volcano (extinct)

◂**Fig. 5** **a** New U–Pb zircon ages, combined with Supakulopas ' (2018) $^{40}Ar/^{39}Ar$ ages and coupling of the schematic, composite stratigraphic column with the geomagnetic polarity time scale. The schematic stratigraphic column (same color legend as in Fig. 2) is based on original fieldwork, integrated with data by Kristjánsson et al. (2004) and Supakulopas (2018) from Mt. Hólafjall. The weighted average plots were made with Isoplot (Ludwig 2012). *TuffZirc* age plots for the two high-MSWD samples are presented in the upper right corner (generated using the *TuffZirc* algorithm of Isoplot by Ludwig and Mundil 2002; detailed in Fig.S3 of the Supplementary Material). **b** Schematic illustration of our new hypothesis; proposed to explain a discrepancy (younging towards west) in the ages of TiCV and ToCV

understanding of the Flateyjarskagi unconformity, the ToCV would be formed in the now extinct SHRZ, while the basalt lavas above the hiatus would be formed in the NVZ. The Flateyjarskagi hiatus appears to span the time from ~ 10 to ~ 6 Ma in the north (i.e., by the peninsula's SE end) and from ~ 7 to ~ 5 Ma in the south (i.e., in the southern part of the Fnjóskadalur valley; Jancin et al. 1985; Cotman 1979; Fig. 1b, c), thus spanning the Miocene-Pliocene boundary (~ 5.3 Ma), while the lavas onlapping the ToCV record ongoing volcanism across this boundary (Figs. 2 and 5a), at least until 5.05 Ma (via stratigraphic correlation with Supakulopas's (2018) $^{40}Ar/^{39}Ar$ ages). On the other hand, the hiatus above the ToCV may simply represent a local break at the end of the volcano's active period. Assuming that the geodynamic setting since the volcano's lifetime until present was dominated by spreading, the distance between the ToCV and the present NVZ (~ 70 km) is consistent with origin within the NVZ and a mean spreading half-rate of ~ 1 cm/year (e.g., Árnadóttir et al. 2008). Furthermore, considering the general assumptions that regional lava dips in Iceland result from loading by voluminous lava flows in the respective volcanic zone (e.g., Pálmason 1973; Pálmason and Sæmundsson 1974; Walker 1960), the regional southeast dip direction of the strata in the ToCV area might be taken to indicate origin within a zone that was roughly coincident with the present NVZ. This would agree with the hiatus representing only a local break and would indicate, as no major hiatuses are present, that a time gap related to a rift relocation is non-existent in the ToCV area. If so, the new U–Pb zircon ages from the ToCV may be considered to provide timing of silicic magma erupted soon after its parent rift relocated, and thereby constrains on the oldest silicic rocks formed at the incipient rift. Similar findings of appreciable silicic material erupting soon after relocation of the parent rift (at ~ 5.4–3.9 Ma) are documented at the Hafnarfjall-Skarðsheiði central volcano in West Iceland which began forming nearly contemporaneously with the relocation of the southern segment of the SHRZ to the WVZ (Banik et al. 2018). However, the age progression (younging to the west) of the E-W aligned ToCV and the 5–6 Ma TiCV remains enigmatic as it conflicts with concepts of unidirectional spreading. Considering the age of the main formation of the TiCV, ~ 5.5 Ma (Hjartarson 2003; 2005), it might be suggested that the TiCV originated inside the NVZ. The problem is that the volcano is 90 km west of the NVZ which would indicate a half spreading rate of 1.7 cm/year (Hjartarson 2009). Therefore, the TiCV appears to have formed outside the NVZ and to the west of the then extinct ToCV. As such, the results of our study do not align with the generally established geotectonic framework (e.g., Sæmundsson 1979; Einarsson 2008). Therefore, to provide an explanation for this discrepancy, we propose a new hypothesis (Fig. 5b).

At ~ 8 Ma, the center of the mantle plume was located just east of the ToCV (an assumption based on Steinthorsson et al. (1985) and Martin et al. (2011)), after having reached a critical distance from the northern segment of the SHRZ, already weakening the lithosphere, resulting in partitioned spreading between the SHRZ and the incipient NVZ. To accommodate this rearrangement, the southern end of the NVZ was linked with the SHRZ by a transverse zone which was the precursor of the MIB. Similar to the present MIB, we propose that this proto-MIB was leaky, i.e., comprising a small component of opening, producing sufficient room for magma to erupt. Volcanic activity at this transverse zone was initially most effective at the east end, at the junction of the proto-MIB with the incipient NVZ, approximately by the center of the mantle plume, then gradually migrated westward—away from the center—resulting in the observed age progression of the Torfufell and Tinná central volcanoes. Lavas from the TiCV may have flowed from the west and reached the area around the ToCV and partly or totally covered the edifice along with lavas from the NVZ flowing from the east. This interpretation requires a ~ 50 km southward migration of the transverse zone with time, from the proto-MIB to the present location of the MIB. While such southward advancement could probably be explained partly by the WNW migration of the tectonic plates relative to the mantle plume, it may also be a result of southward propagation of the new rift zone, similar to the indicated southward migration of the SISZ with propagation of the EVZ (e.g., Einarsson 1991; Khodayar and Franzson 2007; Karson 2017) and northward migration of the TFZ with propagation of the NVZ (e.g., Karson 2017; Karson et al. 2019).

Our hypothesis does have some support from the whole-rock geochemical data that indicate that the rock suite of the ToCV is transitional in nature (i.e., has a transitional character towards alkaline rocks) with basalts that are slightly higher in TiO_2 and K_2O compared to typical rift zone basalts and rhyolites that have higher K_2O and lower FeO than typical rift zone rhyolites (Fig. 3; Tables S1 and S2 of the Supplementary Material). A comparison with the neighboring TiCV shows strong similarities between these two central volcanoes and indicates that basalt to rhyolite products of both volcanoes are, in general, more enriched than typical rift zone magmas (Fig. 3). More

importantly, these two volcanoes feature rhyolites similar to rhyolites associated either with the MIB or those in the propagating EVZ, or even the intraplate ÖVB, while their basalts are similar to those from the junction of the WVZ with the SISZ. Nonetheless, the new hypothesis awaits critical testing that optimally will involve extensive structural mapping along the hypothesized proto-MIB, to seek evidence of potential transform-related structures that may be compared with future collection of isotopic data from zircon crystals and whole rocks of the ToCV and TiCV and may be indicators of petrogenetic environments for silicic magmas at these volcanoes (see Carley et al. 2020). To obtain more robust geometric relationships in the central north region of Iceland, we consider dating of the remaining undated silicic centers in the region to be essential. Dating of additional samples from the TiCV and the two adjacent volcanoes in the Flateyjarskagi peninsula that can confidently confirm their ages would furthermore strengthen the dataset, and a closer look at the Víðidalur central volcano would be of particular interest as recent U–Pb zircon ages (6.3–7.3 Ma; Carley et al. 2020) document silicic magmatism at the SHRZ concurrently with silicic activity at the ToCV.

Conclusions

The U–Pb zircon ages (weighted averages) presented here range from 7.15 ± 0.12 to 6.76 ± 0.02 Ma, indicating that silicic magmatism and volcanism of the Torfufell central volcano extended over ~ 400 kyr. Correlations with previous work predict that the life-span of the central volcano is about or just over 1 Myr, commencing with basaltic volcanism at ~ 7.8–8.0 Ma. A ~ 1 Myr volcanic hiatus is recorded between the uppermost rhyolites of the central volcano and the succeeding basaltic lavas, from 6.76 ± 0.02 to 5.73 ± 0.14 Ma, and although broadly contemporaneous with (but shorter than) the Flateyjarskagi unconformity, we propose that this hiatus represents a local break at the end of the volcano's active period. The new U–Pb age data demonstrate that the silicic portion of the Torfufell central volcano was formed nearly synchronously with a major rift relocation in North Iceland and may provide constraints on the oldest silicic rocks formed at the incipient Northern volcanic zone. After its extinction, the Torfufell central volcano was buried beneath younger formations making up the lava succession above the hiatus. We propose that these younger lavas originated from the large Tinná central volcano in the west as well as from the newly formed NVZ in the east. Our results pertain to a key area in the evolving understanding of the development of crustal accretion in Iceland and underline the extensive room for additional high-quality radiometric dating on silicic activity in the central north region.

Supplementary Information The online version contains supplementary material available at https://doi.org/10.1007/s00445-023-01667-8.

Acknowledgements This work is a part of a PhD thesis that was funded through The Icelandic Research Fund of RANNIS (grant number 174395), Iceland GeoSurvey (ÍSOR), and Akureyri's local power company, Norðurorka. Zircons were separated from the five SIMS dated samples by Geotrack in Australia. Dating on zircons from these samples was carried out at the NordSIM facility in Stockholm, with supervision, guidance, and help with sample preparation from the NordSIM staff: Heejin Jeon, Martin Whitehouse, and Kerstin Lindén. Funding agencies of NordSIM are the Swedish Museum of Natural History, the Swedish Research Council, and the University of Iceland. This is NordSIM contribution number 737. The CA-TIMS dated sample was prepared (including zircon separation, CL imaging, and LA-ICPMS) and dated by Dr. Corey Wall at the Pacific Centre for Isotopic and Geochemical Research (PCIGR) of the University of British Columbia, Canada. BSE imaging and EDS analyzing of zircons using SEM were carried out at the University of Iceland, with supervision and guidance from Enico Bali and Ármann Höskuldsson.

Declarations

Conflict of interest There are no financial interests related to this work. It has only academic benefit and it is a part of a PhD project in the University of Iceland.

References

Árnadóttir T, Geirsson H, Jiang W (2008) Crustal deformation in Iceland: plate spreading and earthquake deformation. Jökull 58:59–74. https://doi.org/10.33799/jokull2008.58.059

Aronson JL, Sæmundsson K (1975) Relatively old basalts from structurally high areas in central Iceland. Earth Planet Sci Lett 28:83–97. https://doi.org/10.1016/0012-821x(75)90077-1

Askew RA, Thordarson T, Gans P, Thompson J, Danyushevsky L (2020) Temporal and spatial evolution of the Neogene age Breiðdalur central volcano through 39Ar/40Ar and U-Pb age determination. J Volcanol Geothermal Res 404:107006. https://doi.org/10.1016/j.jvolgeores.2020.107006

Banik TJ, Miller CF, Fisher CM, Coble MA, Vervoort JD (2018) Magmatic-tectonic control on the generation of silicic magmas in Iceland: constraints from Hafnarfjall-Skarðsheiði volcano. Lithos 318–319:326–339. https://doi.org/10.1016/j.lithos.2018.08.022

Carley TL, Miller CF, Sigmarsson O, Coble MA, Fisher CM, Hanchar JM, Schmitt AK, Economos RC (2017) Detrial zircon resolve

longevity and evolution of silicic magmatism in extinct volcanic centers: a case study from the East Fjords of Iceland. Geosphere 13(5):1640–1663. https://doi.org/10.1130/GES01467.1

Carley TC, Miller CF, Fisher CM, Hanchar JM, Vervoort JD, Schmitt AK, Economos RC, Jordan BT, Padilla AJ, Banik RJ (2020) Petrogenesis of silicic magmas in Iceland through space and time: the isotopic record preserved in zircon and whole rocks. J Geol 128:1–28. https://doi.org/10.1086/706261

Clay PL, Busemann H, Sherlock SC, Baryy TL, Kelley SP, McGarvie DW (2015) 40Ar/39Ar ages and residual volatile contents in degassed subaerial and subglacial glassy volcanic rocks from Iceland. Chem Geol 403:99–110. https://doi.org/10.1016/j.chemgeo.2015.02.041

Cotman RM (1979) Potassium-argon evidence for shifting of the axial rift zone in northern Iceland. Dissertation, Case West Reserve University

Debaille V, Troennes RG, Brandon AD, Waight TE, Graham DW, Lee Cin-Ty A (2009) Primitive off-rift basalts from Iceland and Jan Mayen: OS-isotopic evidence for a mantle source containing enriched subcontinental lithosphere. Geochim Cosmochim Acta 73:3423–3449. https://doi.org/10.1016/j.gca.2009.03.002

Einarsson P (1991) Earthquakes and present-day tectonism in Iceland. Tectonophysics 189:261–279. https://doi.org/10.1016/0040-1951(91)90501-I

Einarsson P (2008) Plate boundaries, rifts and transforms in Iceland. Jökull 58:35–58. https://doi.org/10.33799/jokull2008.58.035

Everts P (1975) Die Geologie von Skagi und der Ost-Küste des Skagafjörður (Nord-Island). Dissertation, Geologischen Instituts der Universität Köln

Fitton JG, Saunders AD, Norry MJ, Hardarson BS, Taylor RN (1997) Thermal and chemical structure of the Iceland plume. Earth Planet Sci Lett 153:197–208. https://doi.org/10.1016/S0012-821X(97)00170-2

Flóvenz ÓG, Tómasson J (1992) Hólsgerði í Eyjafirði - Jarðhitarannsóknir 1991 og 1992 (Report No. OS-92062/HJD-04). National Energy Authority of Iceland. https://gogn.orkustofnun.is/Skyrslur/OS-1992/OS-92062.pdf

Flude S, Burgess R, McGarvie DW (2008) Silicic volcanism at Ljósufjöll, Iceland: insights into evolution and eruptive history from Ar–Ar dating. J Volcanol Geoth Res 169:154–175. https://doi.org/10.1016/j.jvolgeores.2007.08.019

Flude S, McGarvie DW, Burgess R, Tindle AG (2010) Rhyolites at Kerlingarfjöll, Iceland: the evolution and lifespan of silicic central volcanoes. Bull Volcanol 72:523–538. https://doi.org/10.1007/s00445-010-0344-0

Fowler APG, Zierenberg RA (2016) Geochemical bias in drill cutting samples versus drill core samples returned from the Reykjanes Geothermal System, Iceland. Geothermics 62:48–60. https://doi.org/10.1016/j.geothermics.2016.02.007

Garcia S, Arnaud NO, Angelier J, Bergerat F, Homberg C (2003) Rift jump process in Northern Iceland since 10 Ma from 40Ar/39Ar geochronology. Earth Planet Sci Lett 214:529–544. https://doi.org/10.1016/S0012-821X(03)00400-X

Guðmundsdóttir E, Eiríksson J, Larsen G (2011) Identification and definition of primary and reworked tephra in Late Glacial and Holocene marine shelf sediments off North Iceland. J Quat Sci 26(6):589–602. https://doi.org/10.1002/jqs.1474

Guillou H, Vliet-Lanoë BV, Guðmundsson A, Nomade S (2010) New unspiked K-Ar ages of Quaternary sub-glacial and sub-aerial volcanic activity in Iceland. Quat Geochronol 5:10–19. https://doi.org/10.1016/j.quageo.2009.08.007

Gunnarsson B, Marsh BD, Taylor HP (1998) Generation of Icelandic rhyolites: silicic lavas from the Torfajökull central volcano. J Volcanol Geoth Res 83:1–45. https://doi.org/10.1016/S0377-0273(98)00017-1

Hall JR, Allison MS, Papadopoulos MT, Barfod DN, Jones SM (2023) Timing and consequences of Bering Strait opening: new insights from $^{40}Ar/^{39}Ar$ dating of the Barmur Group (Tjörnes beds), northern Iceland. Paleoceanography Paleoclimatol 38:e2022PA004539. https://doi.org/10.1029/2022PA004539

Hardarson BS, Fitton JG (1997) Mechanisms of crustal accretion in Iceland. Geology 24:1043–1046. https://doi.org/10.1130/0091-7613(1997)025%3c1043:MOCAII%3e2.3.CO;2

Hardarson BS, Fitton JG, Ellam RM, Pringle MS (1997) Rift-relocation - a geochemical and geochronological investigation of a palaeo-rift in NW Iceland. Earth Planet Sci Lett 153:181–196. https://doi.org/10.1016/S0012-821X(97)00145-3

Harðarson BS, Fitton GJ, Hjartarson Á (2008) Tertiary volcanism in Iceland. Jökull 58:161–178. https://doi.org/10.33799/jokull2008.58.161

Harðarson BS (1993) Alkalic rocks in Iceland with special reference to the Snæfellsjökull volcanic system. Dissertation, University of Edinburgh

Hildreth W (2007) Quaternary magmatism in the Cascades - geologic perspectives. US Geological Survey Professional Paper 1–125.https://doi.org/10.3133/pp1744

Hjartardóttir ÁR, Einarsson P (2021) Tectonic position, structure, and Holocene activity of the Hofsjökull volcanic system, central Iceland. J Volcanol Geothermal Res 417:107277. https://doi.org/10.1016/j.jvolgeores.2021.107277

Hjartarson Á (2005) The Late Miocene Tinná Central Volcano, North Iceland. Jökull 55:33–48. https://doi.org/10.33799/jokull2005.55.033

Hjartarson Á (2009) Central volcanoes as indicators for spreading rate in Iceland. In: Thordarson T, Self S, Larsen G, Rowland S, Höskuldsson A (eds) Studies in Volcanology: The Legacy of Georg Walker. Special Publications of IAVCEI, Geological Society, London, pp 323–330

Hjartarson Á, Sæmundsson K (2014) Geological map of Iceland. Bedrock Iceland GeoSurvey scale 1:600,000

Hjartarson Á (2003) The skagafjörður unconformity, North Iceland, and its geological history. Dissertation, University of Copenhagen

Hopper JR, Funck T, Stoker MS, Árting U, Peron-Pinvidic G, Doornenbal H, Gaina C (2014) Tectonostratigraphic Atlas of the North-East Atlantic Region, 1st edn. Geological Survey of Denmark-Greenland (GEUS), Copenhagen

Jakobsson SP (1979) Petrology of recent basalts of the Eastern Volcanic Zone, Iceland. Acta Naturalia Islandica 26:1–103. https://doi.org/10.1016/0198-0254(81)91274-7

Jakobsson SP, Jónsson J, Shido F (1978) Petrology of the western Reykjanes peninsula, Iceland. J Petrol 19:669–705

Jakobsson SP, Jónasson K, Sigurðsson IA (2008) The three rock series of Iceland. Jökull 58:117–138. https://doi.org/10.33799/jokull2008.58.117

Jancin M, Young KD, Voight B, Aronson JL, Sæmundsson K (1985) Stratigraphy and K/Ar ages across the west flank of the northeast Iceland axial rift zone, in relation to the 7 MA volcano-tectonic reorganization of Iceland. J Geophys Res 90:9961–9985. https://doi.org/10.1029/JB090iB12p09961

Jeon H, Whitehouse MJ (2015) A critical evaluation of U-Pb calibration schemes used in SIMS zircon geochronology. Geostand Geoanal Res 39(4):443–452. https://doi.org/10.1111/j.1751-908X.2014.00325.x

Jóhannesson H (1980) Jarðlagaskipan og þróun rekbelta á Vesturlandi. Náttúrufræðingurinn 50:13–31

Jóhannesson H (1991) Yfirlit um jarðfræði Tröllaskaga. In: Hjálmarsson AH, Jóhannesson H, Björnsson H, Kristinsson H, Kristinsson M (eds) Árbók 1991 – Fjallendi Eyjafjarðar að vestanverðu II. Iceland Touring Association, Reykjavík, pp 39–56

Karaoğlu Ö, Helvacı C, Ersoy EY (2010) Petrogenesis and 40Ar/39Ar geochronology of the volcanic rocks of the Uşak-Güre basin, western Türkiye. Lithos 119:193–210. https://doi.org/10.1016/j.lithos.2010.07.001

Karson JA (2017) The Iceland plate boundary zone: propagating rifts, migrating transforms, and rift-parallel strike-slip faults. Geochem Geophys Geosyst 18:4043–4054. https://doi.org/10.1002/2017GC007045

Karson JA, Brandsdóttir B, Einarsson P, Sæmundsson K, Farrell JA, Horst AJ (2019) Evolution of migrating transform faults in anisotropic oceanic crust: examples from Iceland. Can J Earth Sci 56(12):1–12. https://doi.org/10.1139/cjes-2018-0260

Khodayar M, Franzson H (2007) Fracture pattern of Thjórsárdalur central volcano with respect to rift-jump and a migrating transform zone in South Iceland. J Struct Geol 29:898–912. https://doi.org/10.1016/j.jsg.2006.11.007

Kristjánsson L, Guðmundsson Á, Harðarson BS (2004) Stratigraphy and paleomagnetism of a 2.9-km composite lava section in Eyjafjörður, Northern Iceland: a reconnaissance study. Int J Earth Sci 93:582–595. https://doi.org/10.1007/s00531-004-0409-4

Kristjánsson L, Jóhannesson H, McDougall I (1992) Stratigraphy, age and paleomagnetism of Langidalur, Northern Iceland. Jökull 42:31–44. https://timarit.is/page/6578337#page/n32/mode/2up

Kuritani T, Yokoyama T, Kitagawa H, Kobayashi K, Nakamura E (2011) Geochemical evolution of historical lavas from Askja Volcano, Iceland. Implications for mechanisms and timescales of magmatic differentiation. Geochim Cosmochim Acta 75:570–587. https://doi.org/10.1016/j.gca.2010.10.009

Lacasse C, Sigurðsson H, Carey SN, Jóhannesson H, Thomas LE, Rogers NW (2007) Bimodal volcanism at the Katla subglacial caldera, Iceland: insight into the geochemistry and petrogenesis of rhyolitic magmas. Bull Volcanol 69:373–399. https://doi.org/10.1007/s00445-006-0082-5

Larsen G, Dugmore A, Newton A (1999) Geochemistry of historical-age silicic tephras in Iceland. Holocene 9:463–471. https://doi.org/10.1191/095968399669624108

Larsen G, Newton AJ, Dugmore AJ, Vilmundardóttir E (2001) Geochemistry, dispersal, volumes and chronology of Holocene silicic tephra layers from the Katla volcanic system, Iceland. J Quat Sci 16:119–132. https://doi.org/10.1002/jqs.587

Larsen G, Eiríksson J, Knudsen KL, Heinemeier J (2002) Correlation of late Holocene terrestrial and marine tephra markers, north Iceland: implications for reservoir age changes. Polar Res 21(2):283–290. https://doi.org/10.3402/polar.v21i2.6489

Le Bas MJ, Le Maitre RW, Streckeisen A, Zanettin B (1986) A chemical classification of volcanic rocks based on the total alkali-silica diagram. J Petrol 27:745–750. https://doi.org/10.1093/petrology/27.3.745

Lee JKW (2015) Ar-Ar and K-Ar Dating. In: Rink WJ, Thompson JW (eds) Encyclopedia of Scientific Dating Methods. Springer Science+Buisness Media Dordrecht, pp 58–73

Ludwig KR, Mundil R (2002) Extracting reliable U-Pb ages and errors from complex populations of zircons from Phanerozoic tuffs. Geochim Cosmochim Acta 66(15A):A463–A463

Ludwig KR (2003) User's manual for isoplot 3.00: a geochronological toolkit for microsoft excel (special publication 4), Berkeley Geochronology Center

Ludwig KR (2012) User's manual for isoplot version 3.75–4.15: a geochronological toolkit for microsoft excel (special publication 5), Berkeley Geochronology Center

Maclennan J, MKenzie D, Gronvöld K, Slater L (2001) Crustal accretion under northern Iceland. Earth Planet Sci Lett 191(3–4):295–310. https://doi.org/10.1016/S0012-821X(01)00420-4

Martin E, Sigmarsson O (2007) Crustal thermal state and origin of silicic magma in Iceland: the case of Torfajökull, Ljósufjöll and Snæfellsjökull volcanoes. Contrib Mineral Petrol 153:593–605. https://doi.org/10.1007/s00410-006-0165-5

Martin E, Paquette JL, Bosse V, Ruffet G, Tiepolo M, Sigmarsson O (2011) Geodynamics of rift-plume interaction in Iceland as constrained by new 40Ar/39Ar and in situ U-Pb zircon ages. Earth Planet Sci Lett 311:28–38. https://doi.org/10.1016/j.epsl.2011.08.03

Mattinson JM (2005) Zircon U-Pb chemical abrasion ("CA-TIMS") method: combined annealing and multi-step partial dissolution analysis for improved precision and accuracy of zircon ages. Chem Geol 220:47–66. https://doi.org/10.1016/j.chemgeo.2005.03.011

Mattsson HB, Óskarsson N (2005) Petrogenesis of alkaline basalts at the tip of a propagating rift: evidence from the Heimaey volcanic centre, south Iceland. J Volcanol Geoth Res 147:245–267. https://doi.org/10.1016/j.jvolgeores.2005.04.004

McGarvie DW, Macdonald R, Pinkerton H, Smith RL (1990) Petrogenetic evolution of the Torfajökull volcanic complex, Iceland II: the role of magma mixing. J Petrol 31:461–481. https://doi.org/10.1093/petrology/31.2.461

McGarvie D, Stevenson J, Burgess R, Tuffen H, Tindle A (2007) Volcano–ice interactions at Prestahnúkur, Iceland: rhyolite eruption during the last interglacial–glacial transition. Ann Glaciol 45:38–47. https://doi.org/10.3189/172756407782282453

Meara RH, Thordarson T, Pearce NJG, Hayward C, Larsen G (2020) A catalogue of major and trace element data for Icelandic Holocene silicic tephra layers. J Quat Sci 35(1–2):122–142. https://doi.org/10.1002/jqs.3173

Nicholson H, Condomines M, Fitton J, Fallick A, Gronvöld K, Rogers G (1991) Geochemical and isotopic evidence for crustal assimilation beneath Krafla: Iceland. J Petrol 32:1005–1020. https://doi.org/10.1093/petrology/32.5.1005

Ogg JG (2020) Geomagnetic polarity time scale. In: Gradstein FM, Ogg JG, Schmitz M, Ogg G (eds) Geologic time scale 2020, Elsevier, 159–192. https://doi.org/10.1016/B978-0-12-824360-2.00005-X

Óladóttir BA, Larsen G, Sigmarsson O (2011) Holocene volcanic activity at Grímsvötn, Bárdarbunga and Kverkfjöll subglacial centres beneath Vatnajokull, Iceland. Bull Volcanol 73:1187–1208. https://doi.org/10.1007/s00445-011-0461-4

Óskarsson N, Steinþórsson S, Sigvaldason GE (1985) Iceland geochemical anomaly: origin, volcanotectonics, chemical fractionation and isotope evolution of the crust. J Geophys Res 90:10011–10025. https://doi.org/10.1029/JB090iB12p10011

Pálmason G (1973) Kinematics and heat flow in a volcanic rift zone with application to Iceland. Geophys J R Astron Soc 33:451–481. https://doi.org/10.1111/j.1365-246X.1973.tb02379.x

Pálmason G, Sæmundsson K (1974) Iceland in relation to the mid-Atlantic ridge. Annu Rev Earth Planet Sci 2:25–50. https://doi.org/10.1146/annurev.ea.02.050174.000325

Pétursson HG (1997) Skriðuhætta í Sölvadal (Report No. NÍ-97009). Icelandic Institute of Natural History. http://hdl.handle.net/10802/7617

Pollock M, Edwards B, Hauksdóttir S, Alcorn R, Bowman L (2014) Geochemical and lithostratigraphic constraints on the formation of pillow-dominated tindars from Undirhlíðar quarry, Reykjanes Peninsula, southwest Iceland. Lithos 200–201:317–333. https://doi.org/10.1016/j.lithos.2014.04.023

Roaldset E (1983) Tertiary (Miocene-Pliocene) interbasalt Sediments, NW- and W-Iceland. Jökull 33:39–56. https://timarit.is/page/6577014#page/n39/mode/2up

Sæmundsson K (1974) Evolution of the axial rifting zone in northern Iceland and the Tjörnes Fracture Zone. Geol Soc Am Bull

85(4):495–504. https://doi.org/10.1130/0016-7606(1974)85%3c495:EOTARZ%3e2.0.CO;2
Sæmundsson K (1979) Outline of the geology of Iceland. Jökull 29:7–28
Sæmundsson K, Kristjánsson L, McDougall I, Watkins ND (1980) K-Ar dating, geological and paleomagnetic study of a 5-km lava succcession in Northern Iceland. J Geophys Res 85:3628–3646. https://doi.org/10.1029/JB085iB07p03628
Sæmundsson K (1978) Fissure swarms and central volcanoes of the neovolcanic zones of Iceland. In: Bowes DR, Leake BE (eds) Crustal Evolution in Northwestern Britain and Adjacent Regions. Geological Journal, Specical Issue, 10: 415–432
Schilling JG (1973) Iceland Mantle Plume: Geochemical Evidence along Reykjanes Ridge. Nature 242:565–571
Selbekk RS, Trönnes RG (2007) The 1362 AD Öræfajökull eruption, Iceland: Petrology and geochemistry of large-volume homogenous rhyolite. J Volcanol Geoth Res 160:42–58. https://doi.org/10.1016/j.jvolgeores.2006.08.005
Sigmarsson O, Martin E, Paquette JL, Bosse V, Geirsson K (2012) Gliðnunarhraði Íslands metinn með aldursgreiningum á megineldstöðvum Austurlands. Náttúrufræðingurinn 82(1–4):105–111
Sigvaldason GE (1979) Rifting, magmatic activity and interaction between acid and basic liquids: the 1875 Askja eruption in Iceland. Tech Rep, Nordic Volcanol Inst 79:03
Sinton J, Grönvold K, Sæmundsson K (2005) Postglacial eruptive history of the Western Volcanic Zone. Icel Geochem Geophys Geosyst 6:Q12009. https://doi.org/10.1029/2005GC001021
Slater L, McKenzie D, Grönvold K, Shimizu N (2001) Melt generation and movement beneath Theistareykir, NE Iceland. J Petrol 42:321–354. https://doi.org/10.1093/petrology/42.2.321
Slater L (1996) Melt generation beneath Iceland. Dissertation, University of Cambridge
Steinthorsson S, Óskarsson N, Sigvaldason GE (1985) Origin of alkali basalts in Iceland: a plate tectonic model. J Geophys Res 90(12):10027–10042. https://doi.org/10.1029/JB090iB12p10027
Supakulopas R (2018) Palaeomagnetic studies of Eyjafjardardalur, northern Iceland: does the geocentric axial dipole exist during 3–7 Ma? Dissertation, Imperial College, London
Tatsumi Y, Suenaga N, Yoshioka S, Kaneko K, Matsumoto T (2020) Contrasting volcano spacing along SW Japan arc caused by difference in age of subducting lithosphere. Nat Sci Rep 10:15005. https://doi.org/10.1038/s41598-020-72173-6
Thordarson T, Höskuldsson Á (2002) Iceland. Classic Geology in Europe 3 (Second Edition). Dunedin, Edinburgh/London
Thordarson T, Höskuldsson Á (2008) Postglacial volcanism in Iceland. Jökull 58:197–228. https://doi.org/10.33799/jokull2008.58.197
Viccaro M, Nicotra E, Urso S (2015) Production of mildly alkaline basalts at complex ocean ridge settings: perspectives from basalts emitted during the 2010 eruption at the Eyjafjallajökull volcano, Iceland. J Geodyn 91:51–64. https://doi.org/10.1016/j.jog.2015.08.004
Vink GE (1984) A hotspot model for the Iceland and Voring plateau. J Geophys Res 89:9949–9959. https://doi.org/10.1029/JB089iB12p09949
Walker GPL (1960) Zeolite zones and dike distribution in relation to the structure of the basalts of eastern Iceland. J Geol 68:515–527. https://doi.org/10.1086/626685
Walker GPL (1963) The Breiddalur central volcano, eastern Iceland. Quart J geol Soc Lond 119:29–63. https://doi.org/10.1144/gsjgs.119.1.0029
Wall CJ, Scoates JS, Weis D, Friedman RM, Amini M, Meurer WP (2018) The stillwater complex: integrating zircon geochronological and geochemical constraints on the age, emplacement history and crystallization of a large, open-system layered intrusion. J Petrol 59:153–190. https://doi.org/10.1093/petrology/egy024
Whitehouse MJ, Kamber BS (2005) Assigning dates to thin gneissic veins in high- grade metamorphic terranes: a cautionary tale from Akilia, southwest Greenland. J Petrol 46:291–318. https://doi.org/10.1093/petrology/egh075
Winchester JA, Floyd PA (1976) Geochemical magma type discrimination application to altered and metamorphosed basic igneous rocks. Earth Planet Sci Lett 28:459–469. https://doi.org/10.1016/0012-821X(76)90207-7
Wolfe CJ, Bjarnason IT, Van Decar JC, Solomon SC (1997) Seismic structure of the Iceland mantle plume. Nature 385:245–247. https://doi.org/10.1038/385245a0
Zierenberg RA, Schiffman P, Barfod GH, Lesher CE, Marks NE, Lowenstern JB, Mortensen AK, Pope EC, Bird DK, Reed MH, Friðleifsson GÓ, Elders WA (2013) Composition and origin of rhyolite melt intersected by drilling in the Krafla geothermal field, Iceland. Contrib Mineral Petrol 165:327–347. https://doi.org/10.1007/s00410-012-0811-z